Binding of human angiogenin inhibits actin polymerization

Pyatibratov, Mikhail G.; Tolkatchev, Dmitri; Plamondon, Josee; Xu, Ping; Ni, Feng; Kostyukova, Alla S.

Publisher's version / Version de l'éditeur:
https://doi.org/10.1016/j.abb.2009.12.024
Archives of biochemistry and biophysics, 495, 1, pp. 74-81, 2010-01-04

Archives of Biochemistry and Biophysics 495 (2010) 74–81

Contents lists available at ScienceDirect

Archives of Biochemistry and Biophysics

journal homepage: www.elsevier.com/locate/yabbi

Original Paper

Binding of human angiogenin inhibits actin polymerization

Mikhail G. Pyatibratov [a,b,*], Dmitri Tolkatchev [c], Josee Plamondon [c], Ping Xu [c], Feng Ni [c], Alla S. Kostyukova [b]

[a] Institute of Protein Research, Russian Academy of Sciences, 142290 Pushchino, Moscow Region, Russia
[b] Department of Neuroscience and Cell Biology, RWJMS–UMDNJ, 675 Hoes Lane, Piscataway, NJ 08854, USA
[c] Biotechnology Research Institute, National Research Council Canada, Montreal, Quebec, Canada H4P 2R2

ARTICLE INFO

Article history:
Received 28 October 2009
and in revised form 25 December 2009
Available online 4 January 2010

Keywords:
Angiogenin
Angiogenesis
Actin
Polymerization

ABSTRACT

Angiogenin is a potent inducer of angiogenesis, a process of blood vessel formation. It interacts with endothelial and other cells and elicits a wide range of cellular responses including migration, proliferation, and tube formation. One important target of angiogenin is endothelial cell-surface actin and their interaction might be one of essential steps in angiogenin-induced neovascularization. Based on earlier indications that angiogenin promotes actin polymerization, we studied the binding interactions between angiogenin and actin in a wide range of conditions. We showed that at subphysiological KCl concentrations, angiogenin does not promote, but instead inhibits polymerization by sequestering G-actin. At low KCl concentrations angiogenin induces formation of unstructured aggregates, which, as shown by NMR, may be caused by angiogenin's propensity to form oligomers. Binding of angiogenin to preformed F-actin does not cause depolymerization of actin filaments though it causes their stiffening. Binding of tropomyosin and angiogenin to F-actin is not competitive at concentrations sufficient for saturation of actin filaments. These observations suggest that angiogenin may cause changes in the cell cytoskeleton by inhibiting polymerization of G-actin and changing the physical properties of F-actin.

Introduction

The mechanism of action of angiogenin, a potent angiogenic factor, is not yet fully understood, but it appears to involve several different pathways from receptor binding on endothelial cells and nuclear transport to activation of proteolytic enzymes and cascades [1,2]. The small, 14 kDa protein is homologous to the much-studied bovine pancreatic RNase A [3] and its ribonucleolytic activity, albeit several orders of magnitude weaker than the ribonucleolytic activity of RNase A [4,5], is essential for its angiogenic effects [6–8] and complemented by a putative receptor binding site located within a non-catalytic region of the protein, comprising residues 58–70 and 108–111 [5,9–11]. This is evidenced by observations that if the receptor binding site is damaged or altered, these variants of angiogenin lack angiogenic functions, while the enzymatic activity remains intact. In addition, when a structurally divergent surface loop (residues 59–73) in homologous non-angiogenic RNase A was replaced with residues 58–70 of angiogenin, the recombinant protein acquired the ability to promote angiogenesis [12]. To date, a few angiogenin-binding proteins have been characterized, including actinin [13], fibulin 1 [14], follistatin [15], a 170 kDa cell surface protein with an unknown amino acid sequence expressed by endothelial cells [16] and actin [17], a protein that plays an essential role in cell movement and morphology.

Angiogenin and actin appear to form a high-affinity complex with an apparent dissociation constant of ~1–10 nM [17–19]. Attempts have been made to identify the actin-binding site on angiogenin [17,18]. For example, replacement of the active-site histidine residues His13 and His114 by alanine did not alter the capacity of angiogenin for actin binding. However, some proteolytically cleaved forms of angiogenin, e.g. at residues 60–61 or 67–68, had considerably reduced affinity for actin, which suggests that actin interacts with angiogenin via the putative receptor binding site [17,18]. The angiogenin/actin complex was found to accelerate the generation of plasmin, while angiogenin itself blocks actin's ability to inhibit the enzymatic activity of plasmin [20], which was proposed as a mechanism for angiogenin to promote invasiveness of endothelial cells [21].

Despite growing evidence for the importance of the angiogenin/actin complex for angiogenesis, little is known about the molecular details of their binding interactions. It was reported that angiogenin promotes actin polymerization [17], however, the experiments were done at low ionic strength conditions only and the structural nature of the formed polymers has not been investigated. Our studies were undertaken to examine how angiogenin binding affects the polymerization of monomeric G-actin in various conditions and whether it binds to F-actin filaments. We used a

* Corresponding author. Address: Institute of Protein Research, Russian Academy of Sciences, 142290 Pushchino, Moscow Region, Russia. Fax: +7 495 632 7871.
E-mail address: bratov@vega.protres.ru (M.G. Pyatibratov).

0003-9861/$ - see front matter © 2010 Elsevier Inc. All rights reserved.
doi:10.1016/j.abb.2009.12.024

variety of biophysical techniques including fluorescence, differential centrifugation and electron microscopy.

Materials and methods

Protein purification

Chicken pectoral muscle skeletal actin was purified from acetone powder as described [22]. G-actin was purified on a Sephacryl S-300 column [23] and was stored in ice. Actin was labeled with pyrenyl-iodoacetamide (Invitrogen Molecular Probes, Eugene, OR), and the labeling yields were calculated according to published procedures [24,25]. The degree of the labeling was 80–99%. Recombinant short non-muscle α-tropomyosin, TM5a, and long striated muscle α-tropomyosin, stTM, purified from chicken muscle tissue were a generous gift from Dr. Sarah Hitchcock-DeGregori (RWJMS, Piscataway, NJ). The actin concentrations were calculated from the UV spectrum using an extinction coefficient of 11.0 (1% at 280 nm). Concentrations of angiogenin and tropomyosin were determined by measuring their difference spectra in 6 M guanidine–HCl between pH 12.5 and 6.0 [26] using the extinction coefficients of 2357 (M^{-1} cm^{-1}) for tyrosine and 830 (M^{-1} cm^{-1}) for tryptophan [27]. Protein purity was evaluated using SDS–PAGE [28].

Unlabeled and ^{15}N-labeled recombinant human angiogenin samples were produced in *Escherichia coli* BL21(DE3) (Novagen) grown in, respectively, LB or M9 medium containing ^{15}N-ammonium sulfate as the sole nitrogen source [29]. The expression plasmid encoding the gene of human angiogenin was a generous gift from Dr. Robert Shapiro of Harvard Medical School. Protein purification was carried out following a modified procedure for the isolation of mouse angiogenins [30]. Briefly, insoluble cell extract obtained from 2 L of cell culture was resuspended and solubilized in 7 M guanidine–HCl, 0.15 M reduced glutathione, 0.1 M Tris–HCl, 2 mM EDTA, pH 8.0, to the final volume of 40 mL, and stirred under nitrogen for 2 h. The supernatant was dialyzed against a 2 L solution of 0.5 M L-arginine–HCl, 0.6 mM oxidized glutathione, pH 8.0 for 24 h, cleared by centrifugation for 30 min, at 10,000 g, and diluted 5-fold with water. The diluted sample (250 mL) was filtered to remove newly formed insolubles, loaded on SP-Sepharose at 10 mL/min, washed with 25 mM Tris–HCl, 0.2 M NaCl, pH 8.0, and eluted with 25 mM Tris–HCl, 0.8 M NaCl, pH 8.0. The protein was purified on a Vydac C4 reverse-phase HPLC column using a 25–45%, 1%/min, acetonitrile gradient in 0.1% TFA. HPLC fractions containing purified angiogenin were dialyzed in a dialysis bag extensively against 20 mM sodium acetate, pH 5.5. The identity of the purified protein was confirmed by mass spectrometry and NMR spectroscopy. The protein samples were stored at 4 °C before use. Immediately before NMR experiments, angiogenin was exchanged into an appropriate buffer using Amicon Centriprep YM-3 filter units.

Fluorescence measurements

Actin polymerization was measured using the change in pyrene–actin fluorescence [24] using a PTI fluorimeter (Lawrenceville, NJ) (excitation, 366 nm and emission, 387 nm, with a 1 nm slit). Polymerization was monitored by the increase in fluorescence when 250 μL of the samples containing 2 μM actin (10% pyrenylactin) in the depolymerization buffer (2 mM Tris, pH 8.0, 0.2 mM $CaCl_2$, 0.2 mM ATP, 0.5 mM dithiothreitol, 1 mM NaN_3) were mixed with an equal volume of angiogenin (0–6 μM) in 2× polymerization buffer (200 mM KCl, 2 mM EGTA, 50 mM imidazole, pH 7.0). The experiments were done both in the presence of 2 mM $MgCl_2$ and the absence of magnesium. In the salt dependence experiments, KCl concentration in the added solutions was varied from 0 to 600 mM. Each sample was prepared in sets of four, and the fluorescence was followed 60 min at 25 °C in parallel in a four-cuvette holder.

Sedimentation experiments

The experimental conditions were the same as in the fluorescence studies, and the polymerization reactions were carried out for 1–2 h before being centrifuged. The interactions of angiogenin and tropomyosin with F-actin were followed for 2 h by the addition of 0.1 M KCl to G-actin (1 μM) at 25 °C. Angiogenin and/or tropomyosin were added to F-actin to the final concentration of 1 μM and incubated for 1–2 h. Reaction mixtures (200 μL) were centrifuged at 100,000 rpm for 20 min at 4 °C. In differential sedimentation studies, samples were progressively pelleted at 15,000, 60,000 and 100,000 rpm for 20 min at 4 °C (TLA-100, Beckman). Protein ratios in the aggregates or polymers were measured by quantifying co-sedimented precipitates. The pellets were suspended in 20 μL of the SDS–PAGE sample buffer and analyzed using SDS–PAGE. The gels were stained with Coomassie R-250, and quantified using a Molecular Dynamics model 300A computing densitometer (Sunnyvale, CA). Mixtures of angiogenin and actin at known ratios were used as controls to transfer density ratios to molar ones.

Electron microscopy

The specimens were prepared by negative staining with 2% uranyl acetate on carbon-coated copper grids. A 20 μL sample drop containing 1–2 μM total protein was placed on the grid for 2 min, blotted with filter paper, and stained with 20 μL 2% uranyl acetate for 1–1.5 min. Excess stain was removed with filter paper, and the grid was air dried. Samples were examined on a Phillips CM12 electron microscope (FEI, Eindhoven, The Netherlands), equipped with a digital camera operating at 120 kV.

NMR experiments

Two-dimensional [^{15}N–^{1}H]-HSQC spectra were recorded in 20 mM sodium acetate buffer, pH 5.0 or 6.8, at 25 °C, using an Avance-800 MHz NMR spectrometer (Bruker). The solvent proton signal was suppressed by a WATERGATE pulse sequence [31]. Intermolecular interactions were followed by the HSQC spectra of ^{15}N-labeled angiogenin titrated with a concentrated solution of unlabeled angiogenin in the same buffer. Assignment of the HSQC spectra was performed as described previously [29].

Results

Influence of angiogenin on G-actin polymerization

The influence of angiogenin on actin polymerization was studied using the pyrene–actin fluorescence assay at several KCl concentrations; a concentration of 1 μM was used for both actin and angiogenin. It is known that G-actin does not polymerize at low ionic strength and increasing concentrations of KCl induce polymerization of actin [32,33]. At low ionic strength, i.e. with 0.01 M KCl, the fluorescence intensity remained constant (filled circles, Fig. 1A), while higher concentrations of KCl induce polymerization of actin reported by an increase in fluorescence intensity. Consistent with [33], doubling the salt concentration from 0.1 to 0.2 M KCl somewhat decreases the fluorescence intensity, as shown in Fig. 1A, filled inverted triangles and filled squares, respectively.

At 0.01 M KCl, the addition of angiogenin at 1:1 angiogenin/actin ratio caused a time-dependent increase of pyrene–actin fluorescence (open circles, Fig. 1A). It should be noted that even though

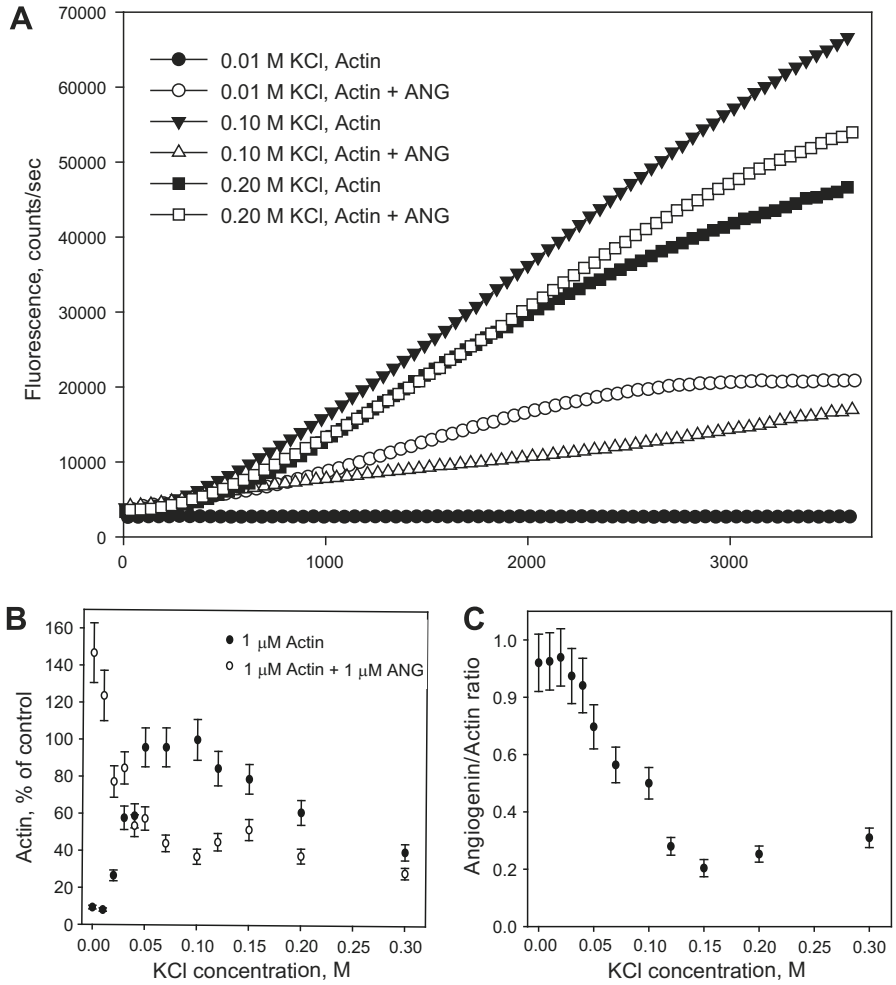

Fig. 1. Influence of angiogenin on actin polymerization at different KCl concentrations. (A) Change in pyrene–actin fluorescence at different KCl concentrations. Black and white symbols – actin (1 μM + 0.1 μM pyrene–actin) without and with angiogenin (1 μM): 0.01 M KCl (circles), 0.10 M KCl (triangles), 0.20 M KCl (squares). (B) Amounts of pelleted actin (100,000 rpm) at different KCl concentrations in the presence (○) and absence (●) of angiogenin. The amount of actin polymerized at a standard condition (0.1 M KCl) was taken as 100%. (C) Angiogenin/actin molar ratio in pellets prepared after sedimentation at 100,000 rpm. Experimental conditions are as described in Materials and methods.

the fluorescence intensity increased appreciably after 1 h, it was still at least 3.5-fold lower than that for actin under the standard conditions of polymerization (0.1 M KCl, no angiogenin). Surprisingly, at 0.05–0.15 M KCl, angiogenin appeared to have the opposite effect and to inhibit normal actin polymerization (open triangles, data shown for 0.1 M KCl). At 0.2 M and higher concentrations of KCl, the presence of angiogenin had very little effect on actin polymerization (open squares).

Next, the actin solutions were centrifuged 2 h after inducing polymerization, and the pellets were analyzed using SDS–PAGE. We found that at 0–0.05 M KCl the amount of actin in pellets formed in the presence of angiogenin is higher than the corresponding amount of actin in the control experiments without angiogenin (Fig. 1B). At higher KCl concentrations (0.05–0.20 M) the amount of actin in the pellets was lower than that in the control experiments. Angiogenin was present in the pellets along with actin, and the angiogenin/actin molar ratio in the pellets depended on the KCl concentration. The maximal ratio was estimated as 1:1, and it was observed in the range of KCl concentrations from 0 to 0.04 M. The angiogenin/actin ratio reduced to approximately 1:2 at 0.05–0.1 M KCl and then decreased to 1:4 at higher KCl concentrations (>0.1 M) (Fig. 1C).

We then used electron microscopy to find out if actin forms filaments when polymerized in the presence of angiogenin. We found that at low ionic strength (0.01 M KCl) actin does not form structured filaments in the presence of angiogenin, and we only observed aggregates that have no regular structure (Fig. 2A and B). Aggregates were not observed in actin preparations without angiogenin. At 0.1 M KCl in the presence of angiogenin, both aggregates and regularly-structured actin filaments were formed (Fig. 2C and D), however, the filaments were significantly shorter than those in control experiments (Fig. 2E) and their number was relatively low.

At angiogenin concentrations lower than 0.2 μM (an angiogenin/actin molar ratio of 1:5) there was a small decrease of actin polymerization induced by 0.1 M KCl, however, the shape of the polymerization curves and the duration of the lag phase were similar to those for actin alone (Fig. 3A). At higher angiogenin concentrations up to 1.0 μM, actin polymerization rates decreased substantially. In addition, inhibition of polymerization in the presence of 1–3 μM angiogenin correlated with the disappearance of the lag phase (Fig. 3A, insert). We believe that this behavior reflects rapid angiogenin binding to actin monomers, leading to the formation of small actin aggregates.

After 1 h, the reaction mixtures were centrifuged and the pellets were analyzed using SDS–PAGE. The resulting data were in a good agreement with those obtained by fluorescence measurements. The amount of actin in the pellets decreased when the angiogenin concentration increased and reached its minimum at 1–3 μM

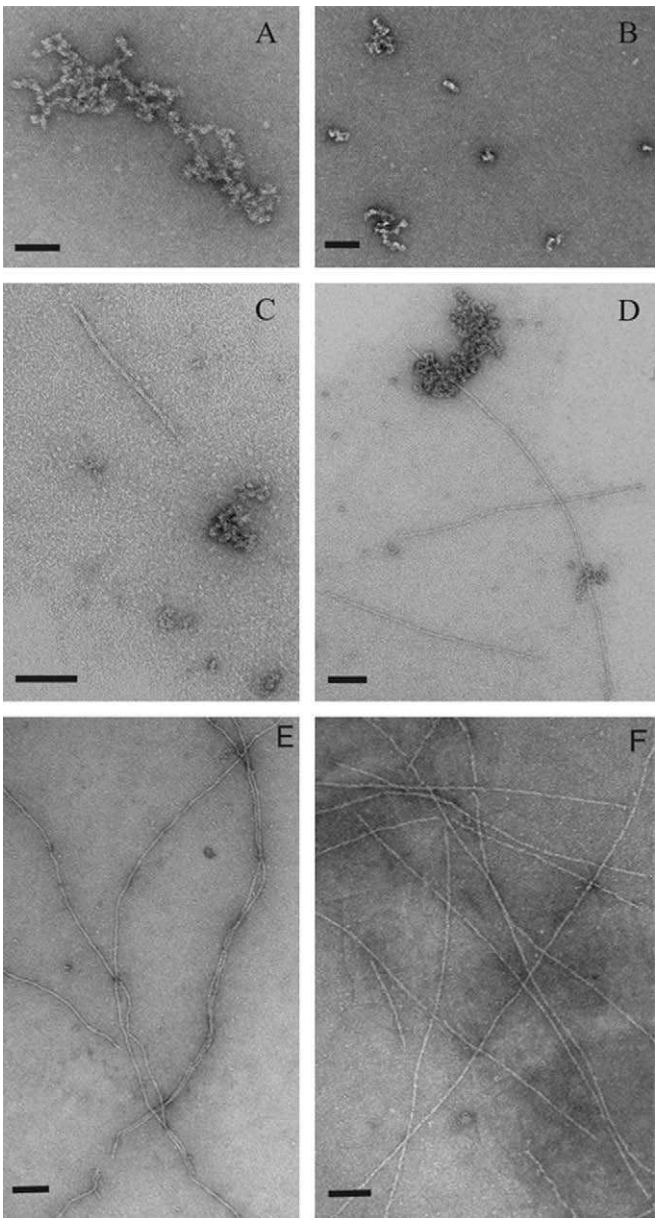

Fig. 2. Electron micrographs of negatively stained samples: angiogenin/actin complexes forming at 0.01 M (A and C) and 0.10 M KCl (B and D); F-actin in 0.10 M KCl without (E) and with (F) angiogenin. The scale bar corresponds to 100 nm.

angiogenin (~40% of the control in the absence of angiogenin) (Fig. 3B). The angiogenin/actin molar ratio in the pellets increased when the angiogenin concentration increased approaching 1:1 stoichiometry (Fig. 3C).

Taken together, these data show that angiogenin does not nucleate polymerization of actin and instead causes the formation of actin aggregates. As a result, angiogenin inhibits actin polymerization under physiological salt conditions by decreasing the concentration of free G-actin.

Interaction of angiogenin with F-actin

We also studied the interaction of angiogenin with preformed F-actin in solutions containing 0.1 M KCl. We found that addition of angiogenin does not depolymerize F-actin but rather binds to the actin filaments. When 1 μM angiogenin was present in an equimolar concentration with F-actin (in monomeric units), an angiogenin/actin molar ratio of ~1:2 was found in the sedimented filaments.

Mixtures of 1 μM F-actin (in G-actin units) and angiogenin were progressively centrifuged at three different speeds (15,000, 60,000 and 100,000 rpm) and pellets were analyzed using SDS–PAGE. We found that when angiogenin was added to F-actin, most of the filaments sedimented at 15,000 rpm (Fig. 4C) while in the absence of angiogenin, F-actin sedimented only at 60,000 rpm (Fig. 4A). When the concentration of angiogenin added to F-actin was below 0.2 μM, we observed no difference in sedimentation properties as compared with the control (data not shown). Interestingly, when actin was polymerized in the presence of angiogenin, similar amounts of actin were sedimented at each of the three speeds (data not shown). We assume that this is caused by high heterogeneity of polymers and aggregates forming under these conditions.

As actin filaments with angiogenin can be sedimented at essentially lower speed we expected that the filaments form bundles. Using EM we did not observe the formation of filament bundles after angiogenin was added, however, there was an obvious change in the appearance of the filaments. When angiogenin was added to F-actin, the filaments appear straighter (Fig. 2F) without noticeable changes in filament width. We hypothesize that binding of a basic angiogenin (pI ~ 9.5) to the negatively-charged F-actin surface may lead to a drastic change of filament net charge. This may cause changes in the solubility and sedimentation behavior of actin filaments.

We tested if the presence of tropomyosin, an actin filament binding protein, can prevent angiogenin binding and vice versa. Tropomyosin binds along both sides of actin filaments and regulates actin depolymerization, severing, polymerization and branching by protecting actin from interaction with other actin binding proteins, such as DNase I, ADF/cofilin, formin and Arp2/3 [34–38]. We expected that tropomyosin would have an effect on angiogenin binding to F-actin. However, at concentrations of tropomyosin and angiogenin sufficient for saturation of actin filaments, independently of the order of mixing, upon the addition of angiogenin, F-actin sediments at 15,000 rpm. In the experiments we used both recombinant TM5a, a short non-muscle α-tropomyosin, which is able to bind F-actin and *N*-acetylated striated muscle long α-tropomyosin (stTM). The results were similar for both tropomyosins (Fig. 4C, D, and I–M). Importantly, both tropomyosin and angiogenin co-sediment with F-actin in either the presence or absence of the second F-actin binding protein, and in all precipitates, the molar ratios of tropomyosin/actin (0.36 ± 0.04 for TM5a and 0.25 ± 0.03 for stTM) and angiogenin/actin (0.91 ± 0.10) did not decrease (Fig. 4C, D, and I–M). Therefore binding of tropomyosin and angiogenin to F-actin appears to be independent and we concluded that these proteins do not share the same binding interface on F-actin. However, when we decreased the angiogenin concentration, filaments also precipitated at 15,000 rpm but in case when tropomyosin was added first part of filaments precipitated at 60,000 rpm (Fig. 4B–H). These filaments co-precipitated with tropomyosins but only trace amounts of angiogenin were seen in the pellets. Further decrease of angiogenin concentration increased the amount of F-actin that precipitated at 60,000 rpm (data not shown).

NMR studies of intermolecular interaction of angiogenin

Angiogenin is a member of the pancreatic ribonuclease superfamily and is structurally homologous to bovine pancreatic RNase A [3]. Interestingly, RNase A has been shown to form a dimeric structure by means of 3D domain swapping, which can lead to the formation of linear oligomers [39]. We examined whether angiogenin can also dimerize in solution and if the ability of angiogenin to promote actin aggregation may be related to the formation of angiogenin dimers and possibly higher-order oligomers.

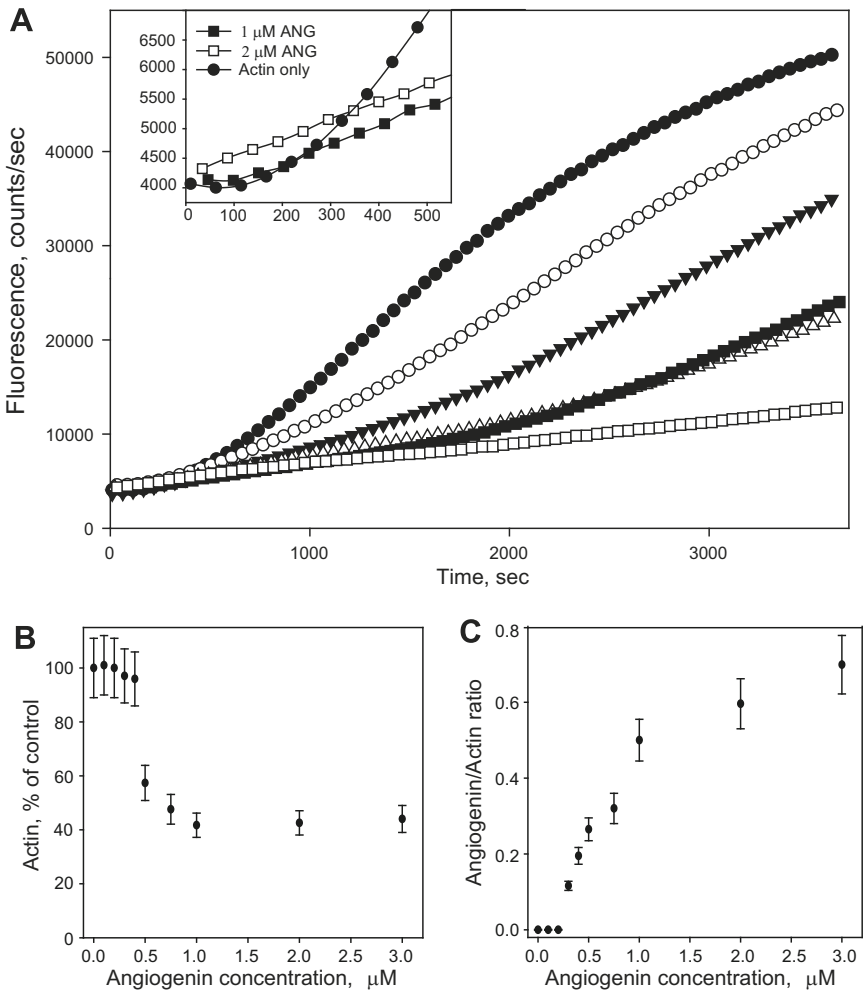

Fig. 3. Influence of different angiogenin concentrations on actin polymerization at 0.1 M KCl: (A) Change in pyrene–actin fluorescence (1 μM actin + 0.1 μM pyrene–actin) without (●) and with angiogenin: 0.2 μM (○), 0.4 μM (▼), 0.5 μM (▽), 1.0 μM (■), and 2.0 μM (□). Inset shows initial stage of polymerization. (B) Amounts of pelleted actin (100,000 rpm) at different angiogenin concentrations. Amount of actin polymerized without angiogenin was taken as 100%. (C) Angiogenin/actin molar ratio in pellets prepared after sedimentation at 100,000 rpm. Experimental conditions are as described in Materials and methods.

We first titrated a sample of ^{15}N-labeled angiogenin at a low concentration of 50 μM and a pH of 5.0 with unlabeled angiogenin and followed the [^{15}N–^{1}H]-HSQC spectra up to 0.25 mM for the total concentration of ^{15}N-labeled and unlabeled angiogenin.

Very interestingly, some HSQC peaks at pH 5.0 were found to depend on the concentration of angiogenin with several selected cross-peaks significantly affected by the addition of unlabeled angiogenin (Fig. 5A). The perturbed peaks exhibited resonance shifts but did not show detectable broadening, indicating that the kinetic exchange processes between free angiogenin molecules and those involved in intermolecular interactions are fast on the NMR chemical-shift time scale. Limited peak shifts suggest weak

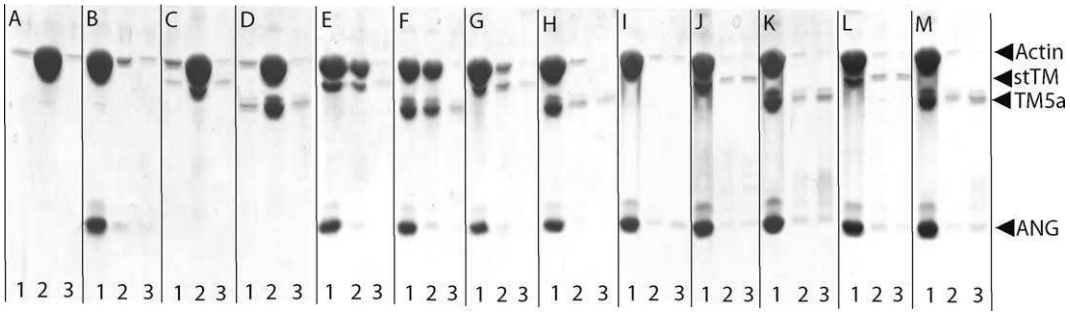

Fig. 4. Co-sedimentation of angiogenin with F-actin. (1, 2, 3) – pellets prepared after three progressive centrifugation cycles, at 15,000, 60,000 and 100,000 rpm, respectively: (A) actin (1 μM) was polymerized at 0.1 M KCl; (B) 1 μM angiogenin was added to F-actin; (C) 1 μM tropomyosin stTM was added to F-actin; (D) 1 μM tropomyosin TM5a was added to F-actin; (E and F) 1 μM stTM (TM5a) and then 1 μM ANG were added to the F-actin; (G and H) 1 μM ANG and then 1 μM stTM (TM5a) were added to F-actin; (I) 2 μM angiogenin was added to F-actin; (J and K) 1 μM stTM (TM5a) and then 2 μM ANG were added to the F-actin; (L and M) 2 μM ANG and then 1 μM stTM (TM5a) were added to F-actin. Experimental conditions are as described in Materials and methods.

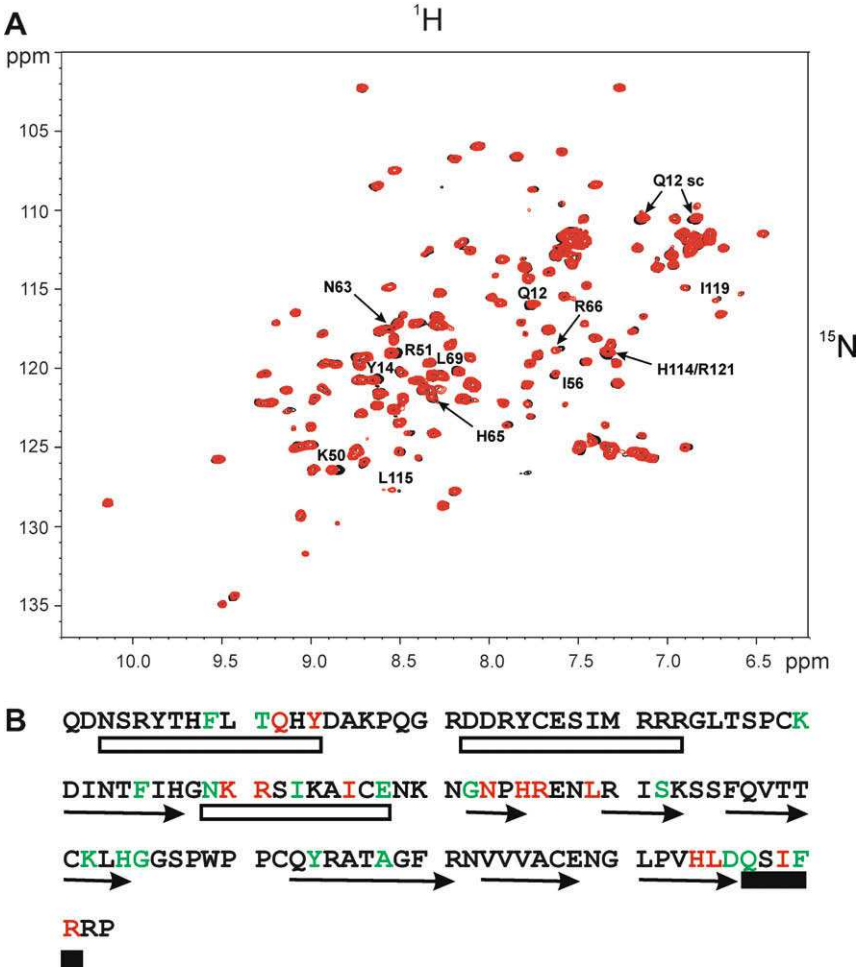

Fig. 5. Intermolecular interactions of angiogenin probed by use of NMR spectroscopy. (A) Shown in red is the [^{15}N–H]-HSQC spectrum of 50 μM ^{15}N-angiogenin in 20 mM CH_3COONa, 0.01% NaN_3 at pH 5.0, 10% D_2O and 298 K. Superimposed (in black) is the HSQC spectrum of the same sample of ^{15}N-angiogenin after the addition of unlabeled angiogenin to a concentration of 204 μM. Indicated are residues which are shifted by >9 Hz upon addition of unlabeled angiogenin. Shifts δ (Hz) were calculated using the expression $\delta^2 = (\delta(^1H))^2 + (\delta(^{15}N) \times \alpha_N)^2$, where the scale factor $\alpha_N \sim 0.866$ was estimated as a ratio of ^{1}H and ^{15}N spectral dispersions for the backbone resonances of angiogenin [49]. (B) Residues of angiogenin involved in intermolecular interactions. Residues in green and red are those whose HSQC peaks (6A) are shifted by >5 and >9 Hz upon addition of unlabeled angiogenin, respectively. Elements of secondary structure are shown as open rectangles (α-helices), arrows (β-strands) and a black rectangle (3_{10}-helix) [50]. (For interpretation of the references to color in this figure legend, the reader is referred to the web version of this article.)

intermolecular associations with a dissociation constant in the sub-millimolar (or high micromolar) range.

Fig. 5B shows the residues of angiogenin with shifted [^{15}N–^{1}H]-HSQC peaks and their locations relative to the secondary structure elements. The majority of the most affected residues (marked as "red") are located in the first and third α-helices, the second β-strand and in the C-terminal segment of the protein consisting of a β-strand and a 3_{10}-helix (Fig. 5B). However, some of these shifted peaks were also very pH-sensitive, and their shifts may be largely caused by otherwise undetectable pH variations (<0.05 pH units) in the course of adding unlabeled angiogenin. To remove this possible ambiguity, we then followed the dependence of the angiogenin [^{15}N–^{1}H]-HSQC spectra on the change of pH from 5.0 to 6.8 (data not shown). It can be concluded with certainty that resonance shifts of at least residues Tyr14, Lys50, Arg51, His65, Leu115 and Ile119 are all caused primarily by concentration changes upon addition of unlabeled angiogenin, as the HSQC peaks of these residues exhibited little pH sensitivity to the pH variation.

Very importantly, at pH 6.8, the same residues Tyr14, Lys50, Arg51 and His65 exhibiting concentration-dependent resonance shifts at pH 5.0 (Fig. 5) became significantly broadened to the extent that they were no longer observable. At the same time, the vast majority of [^{15}N–^{1}H]-HSQC peaks remained sharp and clearly visible, both at a low concentration of 50 μM and at 0.3 mM of ^{15}N-labeled angiogenin. When unlabeled angiogenin was added to the low-concentration ^{15}N-labeled sample, the relatively sharp amide resonance of Leu115 in the HSQC spectra demonstrated a marked dependence on the concentration of unlabeled angiogenin, similar to that observed at pH 5.0. In all, intermolecular interactions of angiogenin appear to be even more pronounced at a near neutral pH of 6.8 than at pH 5.0, manifesting differential line broadening for residues involved in binding down to a very low concentration (~50 μM) of angiogenin.

Discussion

A large number of proteins bind to actin and participate in essential cellular functions, including cell motility, cytokinesis, maintenance of cell structure and organelle movement [40]. The direct interaction between angiogenin and actin [17–19] has been implicated in re-modeling of the extracellular matrix (ECM)[1] and the degradation of basement membrane, therefore promoting cell invasion into the perivascular tissue [21]. However, the interpreta-

[1] *Abbreviation used:* ECM, extracellular matrix.

tion of the interaction between actin and angiogenin was based only on the increased turbidity and the formation of actin sediments promoted by angiogenin in the absence of KCl and Mg^{2+} essential for actin polymerization [17]. In agreement with these experimental findings, we observed an angiogenin-induced increase of pyrene–actin fluorescence at low ionic strength. Using EM, we found that actin did not form regular filaments, but rather unstructured aggregates with a 1:1 ratio in the content of actin/angiogenin. The unstructured aggregates explain the decreased total fluorescence intensity of the "polymerized" actin in comparison with F-actin; since all or a portion of fluorescent pyrenyl moieties may experience a different local environment.

The ability of angiogenin to aggregate actin may be related to the tendency of angiogenin to dimerize and possibly to form higher-order oligomers in solution, as shown by the dependence of the [^{15}N–^{1}H]-HSQC spectrum on the concentration of angiogenin (Fig. 5). The rate of exchange between the interacting species is fast on the NMR time scale, and the NMR peak shifts indicate an apparent dissociation constant in the high μM range. Superficially, this interaction may appear to be too weak to affect the process of actin polymerization, but angiogenin–angiogenin affinity may change considerably upon the formation of the actin/angiogenin complex. There is also the possibility of strong multivalent angiogenin–angiogenin interactions between angiogenin molecules immobilized on oligomerized actin. Interestingly, the homologous RNase A has been demonstrated to dimerize by three-dimensional domain swapping of either the N-terminal helix [41] or its C-terminal β-strand and to form higher-order, possibly amyloid-like, aggregates [39]. Consistently, we observed that many residues affected by the increase in the angiogenin concentration are localized in the first α-helix and at the C-terminus. The underlying RNase A–RNase A interaction is also weak and an apparent dissociation constant in solution was estimated as ~2 mM [42], similar to what we observed for angiogenin. There is therefore also the possibility that oligomerized actin may promote the formation of amyloid-like aggregates as part of the actin aggregation process in the presence of angiogenin.

Whereas, at low ionic strength, angiogenin promotes the aggregation of actin, addition of angiogenin under physiological salt conditions (~0.1 M KCl) has a different effect; it inhibits the formation of structured filaments normally formed by G-actin. In the presence of angiogenin, the amount of actin sedimented was much lower than that in control experiments (without angiogenin) and the pellet contained both unstructured aggregates and short F-actin filaments. On the other hand, if the F-actin filaments were preformed before angiogenin was added, no depolymerization was observed upon binding angiogenin (Fig. 2E and F). Rather, the appearance of the preformed filaments changed in the presence of angiogenin and showed an apparent filament straightening, implying an increase in mechanical stiffness (Fig. 2E and F). The biological significance of this effect of angiogenin is not clear but mechanical properties of both the actin cytoskeleton and the extracellular matrix are known to have profound effects on cell structure and function [43,44], on tissue morphogenesis [45] as well as on the angiogenic process [46].

Based on our data, at saturating concentrations of angiogenin, tropomyosin has no effect on angiogenin binding to F-actin as well as angiogenin has no effect on binding tropomyosin to F-actin. At lower concentrations of angiogenin, tropomyosin prevents binding of angiogenin and is able to protect at least part of actin filaments. However, if angiogenin was added first, tropomyosin is unable to remove it from the filaments. Tropomyosin regulates many actin properties including stabilization of actin filaments. For example, in epithelial cells, short non-muscle tropomyosin, Tm5a, is associated with actin filaments that regulate the insertion and/or retention of a membrane transporter into the plasma membrane, and therefore can regulate the activity of the transporter [47]. The inability of tropomyosin to completely prevent angiogenin binding may be crucial for the function of actin filaments associated with membranes. Given the appreciation of the role of mechanical control in development [45] and mechanotransduction in biology and physiology [48], angiogenin-induced stiffening of F-actin, if it also occurs *in vivo*, will add a novel pathway for the multifaceted functions of angiogenin hitherto attributed solely to either the ribonucleolytic activity or other biochemical functions of angiogenin.

In all, we suggest that binding of angiogenin to G-actin as well as to F-actin may cause changes in the cell cytoskeleton by inhibiting the polymerization of G-actin and changing the physical properties of F-actin.

Acknowledgments

We thank Dr. Sarah Hitchcock-DeGregori (RWJMS–UMDNJ) for TM5a and stTM, Dr. Robert Shapiro (Harvard Medical School) for the expression plasmid encoding human angiogenin, and Dr. Raj Patel for help in electron microscopy studies. Supported by the NIH (GM081688) and the UMDNJ Foundation grants to A.S.K., and by the Government of Canada (NRCC Publication No. 50674).

References

[1] A. Tello-Montoliu, J.V. Patel, G.Y. Lip, J. Thromb. Haemost. 4 (2006) 1864–1874.
[2] X. Gao, Z. Xu, Acta Biochim. Biophys. Sin. (Shanghai) 40 (2008) 619–624.
[3] R.T. Raines, Chem. Rev. 98 (1998) 1045–1066.
[4] R. Shapiro, J.F. Riordan, B.L. Vallee, Biochemistry 25 (1986) 3527–3532.
[5] J.W. Harper, B.L. Vallee, Biochemistry 28 (1989) 1875–1884.
[6] R. Shapiro, E.A. Fox, J.F. Riordan, Biochemistry 28 (1989) 1726–1732.
[7] R. Shapiro, B.L. Vallee, Biochemistry 28 (1989) 7401–7408.
[8] T.P. Curran, R. Shapiro, J.F. Riordan, Biochemistry 32 (1993) 2307–2313.
[9] T.W. Hallahan, R. Shapiro, D.J. Strydom, B.L. Vallee, Biochemistry 31 (1992) 8022–8029.
[10] T.W. Hallahan, R. Shapiro, B.L. Vallee, Proc. Natl. Acad. Sci. USA 88 (1991) 2222–2226.
[11] R. Shapiro, B.L. Vallee, Biochemistry 31 (1992) 12477–12485.
[12] R.T. Raines, M.P. Toscano, D.M. Nierengarten, J.H. Ha, R. Auerbach, J. Biol. Chem. 270 (1995) 17180–17184.
[13] H. Hu, X. Gao, Y. Sun, J. Zhou, M. Yang, Z. Xu, Biochem. Biophys. Res. Commun. 329 (2005) 661–667.
[14] H. Zhang, X. Gao, C. Weng, Z. Xu, Acta Biochim. Biophys. Sin. (Shanghai) 40 (2008) 375–380.
[15] X. Gao, H. Hu, J. Zhu, Z. Xu, FEBS Lett. 581 (2007) 5505–5510.
[16] G.F. Hu, J.F. Riordan, B.L. Vallee, Proc. Natl. Acad. Sci. USA 94 (1997) 2204–2209.
[17] G.F. Hu, D.J. Strydom, J.W. Fett, J.F. Riordan, B.L. Vallee, Proc. Natl. Acad. Sci. USA 90 (1993) 1217–1221.
[18] G.F. Hu, S.I. Chang, J.F. Riordan, B.L. Vallee, Proc. Natl. Acad. Sci. USA 88 (1991) 2227–2231.
[19] S.I. Chang, S.B. Paik, S.H. So, B.C. Ahn, J. Biochem. Mol. Biol. 29 (1996) 353–358.
[20] G.F. Hu, J.F. Riordan, Biochem. Biophys. Res. Commun. 197 (1993) 682–687.
[21] G. Hu, J.F. Riordan, B.L. Vallee, Proc. Natl. Acad. Sci. USA 91 (1994) 12096–12100.
[22] J.A. Spudich, S. Watt, J. Biol. Chem. 246 (1971) 4866–4871.
[23] S. MacLean-Fletcher, T.D. Pollard, Biochem. Biophys. Res. Commun. 96 (1980) 18–27.
[24] T. Kouyama, K. Mihashi, Eur. J. Biochem. 114 (1981) 33–38.
[25] J.A. Cooper, S.B. Walker, T.D. Pollard, J. Muscle Res. Cell Motil. 4 (1983) 253–262.
[26] H. Edelhoch, Biochemistry 6 (1967) 1948–1954.
[27] G.D. Fasman, in: G.D. Fasman (Ed.), Practical Handbook of Biochemistry and Molecular Biology, CRC Press, Boca Raton, FL, 1989.
[28] U.K. Laemmli, Nature 227 (1970) 680–685.
[29] K. Tonan, P. Xu, J.L. Jenkins, A. Russo, R. Shapiro, F. Ni, Biochemistry 42 (2003) 11137–11149.
[30] D.E. Holloway, M.C. Hares, R. Shapiro, V. Subramanian, K.R. Acharya, Protein Expr. Purif. 22 (2001) 307–317.
[31] V. Sklenar, M. Piotto, R. Leppik, V. Saudek, J. Magn. Reson. Ser. A 102 (1993) 241–245.
[32] F.B. Straub, Stud. Inst. Med. Chem. Univ. Szeged 2 (1942) 3–15.
[33] H. Strzelecka-Golaszewska, E. Prochniewicz, E. Nowak, S. Zmorzynski, W. Drabikowski, Eur. J. Biochem. 104 (1980) 41–52.
[34] S.E. Hitchcock, L. Carisson, U. Lindberg, Cell 7 (1976) 531–542.
[35] S. Ono, K. Ono, J. Cell Biol. 156 (2002) 1065–1076.
[36] T.B. Kuhn, J.R. Bamburg, Adv. Exp. Med. Biol. 644 (2008) 232–249.

[37] L. Blanchoin, T.D. Pollard, S.E. Hitchcock-DeGregori, Curr. Biol. 11 (2001) 1300–1304.
[38] B. Wawro, N.J. Greenfield, M.A. Wear, J.A. Cooper, H.N. Higgs, S.E. Hitchcock-DeGregori, Biochemistry 46 (2007) 8146–8155.
[39] Y. Liu, G. Gotte, M. Libonati, D. Eisenberg, Nat. Struct. Biol. 8 (2001) 211–214.
[40] C.G. dos Remedios, D. Chabara, M. Kekic, I.V. Dedova, M. Tsubakihara, D.A. Berry, N.J. Nosworthy, Physiol. Rev. 83 (2003) 433–473.
[41] Y. Liu, P.J. Hart, M.P. Schlunegger, D. Eisenberg, Proc. Natl. Acad. Sci. USA 95 (1998) 3437–3442.
[42] C. Park, R.T. Raines, Protein Sci. 9 (2000) 2026–2033.
[43] P.A. Janmey, Physiol. Rev. 78 (1998) 763–781.
[44] P.A. Janmey, J.P. Winer, M.E. Murray, Q. Wen, Cell Motil. Cytoskeleton 66 (2009) 597–605.
[45] P. Patwari, R.T. Lee, Circ. Res. 103 (2008) 234–243.
[46] A. Mammoto, K.M. Connor, T. Mammoto, C.W. Yung, D. Huh, C.M. Aderman, G. Mostoslavsky, L.E. Smith, D.E. Ingber, Nature 457 (2009) 1103–1108.
[47] P.W. Gunning, G. Schevzov, A.J. Kee, E.C. Hardeman, Trends Cell Biol. 15 (2005) 333–341.
[48] N. Wang, J.D. Tytell, D.E. Ingber, Nat. Rev. Mol. Cell Biol. 10 (2009) 75–82.
[49] B.T. Farmer 2nd, K.L. Constantine, V. Goldfarb, M.S. Friedrichs, M. Wittekind, J. Yanchunas Jr., J.G. Robertson, L. Mueller, Nat. Struct. Biol. 3 (1996) 995–997.
[50] K.R. Acharya, R. Shapiro, S.C. Allen, J.F. Riordan, B.L. Vallee, Proc. Natl. Acad. Sci. USA 91 (1994) 2915–2919.